

## Fusion cross-section in the ${}^4,6\text{He} + {}^{64}\text{Zn}$ collisions around the Coulomb barrier

M. FISICHELLA(\*)

*Dipartimento di Fisica, Università di Messina - Messina, Italy*  
*INFN, Laboratori Nazionali del Sud - Catania, Italy*

(ricevuto il 31 Dicembre 2010; revisionato il 5 Marzo 2011; approvato il 5 Marzo 2011; pubblicato online il 2 Agosto 2011)

**Summary.** — The halo structure is expected to influence the reaction mechanisms in nuclear collisions. The aim of the experiment discussed in the present paper is to compare the fusion excitation functions for the systems  ${}^6\text{He} + {}^{64}\text{Zn}$  and  ${}^4\text{He} + {}^{64}\text{Zn}$ , in order to investigate the effects of the  ${}^6\text{He}$  two-neutron halo structure on the fusion reaction mechanism at energies around the Coulomb barrier. In particular, new fusion cross-sections for the  ${}^4\text{He} + {}^{64}\text{Zn}$  systems at sub-barrier energies were measured to cover the same energy region of our previous measurements for  ${}^6\text{He} + {}^{64}\text{Zn}$ . The fusion cross-section was measured by using an activation technique. We have observed an enhancement of the fusion cross-section in the reaction induced by  ${}^6\text{He}$  when compared to the one induced by  ${}^4\text{He}$  on the same  ${}^{64}\text{Zn}$  target.

PACS 25.60.-t – Reactions induced by unstable nuclei.

PACS 25.60.Pj – Fusion reactions.

### 1. – Introduction

In the last years, many studies concerning nuclear collisions at energies around and below the Coulomb barrier have been performed to understand the role of the nuclear structure on the reaction mechanisms. The interest on this topic arose with the development of radioactive ion beams (RIBs) which allowed the study of the reactions induced by unstable nuclei and, in particular, by halo nuclei, like  ${}^6\text{He}$ ,  ${}^{11}\text{Li}$ ,  ${}^{11}\text{Be}$ ,  ${}^{19}\text{C}$  or  ${}^8\text{B}$ . These nuclei are characterized by a well-bound core and by a low binding energy of the outer nucleons which occupy single-particle states having low angular momentum ( $s$  or  $p$ ). The corresponding single-particle wave function of these valence nucleons extends mostly outside the potential well. A lot of experimental and theoretical studies have been performed in order to investigate on the effects of the projectile halo structure

(\*) E-mail: [fisichella@lns.infn.it](mailto:fisichella@lns.infn.it)

on reaction mechanisms around the barrier (see, *e.g.*, [1]). Most authors agree that direct processes are favoured because of the low binding energies of the valence nucleons and their extended tails, however, contradictory effects on the fusion cross-section have been predicted. A possible way to approach the problem is to consider the combination of two kinds of effects due to the presence of a halo projectile on the fusion mechanism: static and dynamic effects. The first ones are due to the long range of the radial wave function associated with the valence orbitals; the second ones are due to the coupling of the relative motion of projectile and target to their intrinsic excitations or to the other reactions channels including the breakup. Static effects generate a reduction of the Coulomb barrier and therefore by taking only them into account one should expect an enhancement of the fusion cross-section around and below the barrier. The role of dynamic effects has been investigated using Coupled Channel (CC) calculations including the coupling not only to the bound but also to the continuum states (break-up states). These Continuum-Discretised Coupled Channel (CDCC) calculations [2, 3] predict an enhancement of the sub-barrier complete fusion cross-section and a suppression above it with respect to single barrier calculations. However, the calculated cross-sections and hence the amount of sub-barrier enhancement, depend upon the adopted approximations and the phase space in the continuum considered.

Different theoretical approaches, based on a time-dependent wave packet formalism, which uses a three-body model (core, halo and target) [4], lead to opposite results: the fusion cross-section in the neutron halo case is expected to be slightly suppressed with respect to the non-halo case.

From the experimental point of view low-energy reaction studies with halo nuclei are difficult for the low beam currents and for the low cross-sections of some reaction channel especially below the barrier.  ${}^6\text{He}$  beams are available in several radioactive beam facilities with good intensities (up to  $10^7$  pps) and for this reason fusion reactions induced by this halo nucleus are the most studied of any involving light radioactive beams.

The  ${}^6\text{He} + {}^{209}\text{Bi}$  fusion excitation function has been measured at the University of Notre Dame [5, 6] using an activation technique by detecting the  $\alpha$  particles emitted in the decay of the evaporation residues. An enhancement of the sub-barrier fusion with respect to a single barrier penetration [5, 6] and also to fusion induced by  ${}^4\text{He}$  onto the same  ${}^{209}\text{Bi}$  target [7] is observed.

The fusion reactions  ${}^{4,6}\text{He} + {}^{238}\text{U}$ , were measured in Louvain-la-Neuve [8], by detecting the two fission fragments in coincidence. An enhancement of the fission cross-section for the  ${}^6\text{He}$  case with respect to the  ${}^4\text{He}$  one has been observed. However the analysis of the light particles, emitted in coincidence with the fission fragments, allowed to conclude that the observed fission enhancement is due to transfer-fission events whereas no suppression/enhancement effects are observed in the comparison of the fusion-fission excitation functions for the two systems.

The fusion excitation functions of  ${}^6\text{He}$  and  ${}^8\text{He}$  on  ${}^{197}\text{Au}$  were measured in Dubna [9] and in Ganil [10], respectively, by using activation techniques. An enhancement of the sub-barrier fusion cross-section for the  ${}^6\text{He}$ - and  ${}^8\text{He}$ -induced reactions is observed with respect to the one induced by  ${}^4\text{He}$  on the same target [10]. Both experiments have shown that the cross-section for neutron transfer is much larger than the fusion one below and around the barrier.

Fusion for the system  ${}^{11}\text{Be} + {}^{209}\text{Bi}$  has been measured at RIKEN [11] by detecting the characteristic alpha particles emitted in the evaporation residue decay, as well as fission fragments. The fusion cross-section data, for the  ${}^{11}\text{Be}$ -induced collision were compared with those for the well-bound  ${}^{10}\text{Be}$  nucleus and for the weakly bound  ${}^9\text{Be}$

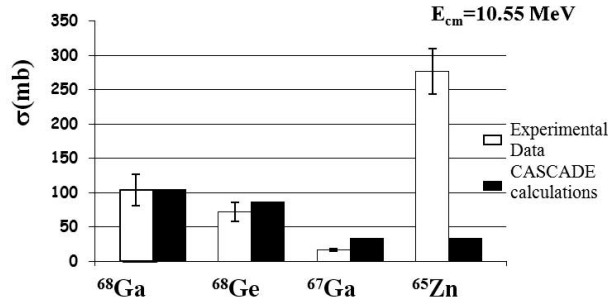


Fig. 1. – Comparison of the experimental cross-sections of the evaporation residues (white histogram) with the prediction of CASCADE calculations (black histogram).

nucleus impinging on the same target. The fusion excitation functions reported in [11] for the three reactions  ${}^9,{}^{10},{}^{11}\text{Be} + {}^{209}\text{Bi}$  show no difference within the errors.

In summary, apparently contradictory conclusions on the presence of enhancement/suppression effects on fusion excitation functions around the barrier in collisions induced by halo nuclei, have been reached by various authors and new experimental data, especially below the barrier, are needed to further investigate this topic.

## 2. – The ${}^6\text{He} + {}^{64}\text{Zn}$ experiment

In a previous study, we measured elastic scattering, direct reactions and fusion for the systems  ${}^4,{}^6\text{He} + {}^{64}\text{Zn}$  at the radioactive beam facility of Louvain-la-Neuve [12, 13] aiming to investigate on the effects of the  ${}^6\text{He}$  halo structure on the reaction mechanisms at energies around the Coulomb barrier. To measure the fusion cross-sections we used an activation technique based on the off-line measurement of the atomic X-ray emission following the electron capture decay of the evaporation residues produced in the reaction. This technique will be discussed more in detail in the next paragraph. The experimental set-up is extensively described in [12]. Stacks of four  ${}^{64}\text{Zn}$  targets, each followed by a  ${}^{93}\text{Nb}$  catcher, were irradiated with  ${}^6\text{He}$  and  ${}^4\text{He}$  beams in order to measure different points in the fusion excitation functions with a single beam energy. The fusion cross-sections were obtained by summing up the cross-sections of all evaporation channels. By comparing the excitation functions for heavy residue production of the two systems an enhancement of the cross-section for the reaction induced by the halo nucleus  ${}^6\text{He}$  was observed when compared to the collision induced by  ${}^4\text{He}$ . Since the same heavy residues can be produced by fusion evaporation but also by other reaction processes, we performed a comparison of the measured cross-section for the different channels with statistical-model calculations [12]. Figure 1 shows the comparison between the experimental cross-section for each heavy residue produced in the  ${}^6\text{He} + {}^{64}\text{Zn}$  reaction and statistical-model predictions for evaporation residues formed in the decay of the compound nucleus  ${}^{70}\text{Ge}$  obtained with the CASCADE code at a center-of-mass energy of about 10.5 MeV.

A good agreement for all the products is observed, with the exception of  ${}^{65}\text{Zn}$  where a large enhancement with respect to the calculation was observed. A possible explanation for the much larger experimental yield of  ${}^{65}\text{Zn}$  with respect to the calculated one could be that other reaction mechanisms are contributing to this particular channel. Indeed, as explained in detail in [12], the  ${}^{65}\text{Zn}$  is formed not only in the fusion-evaporation

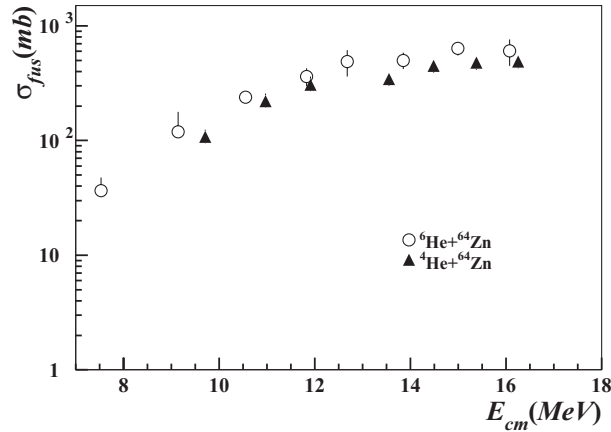


Fig. 2. –  ${}^4\text{He} + {}^{64}\text{Zn}$  (triangles) and  ${}^6\text{He} + {}^{64}\text{Zn}$  (open circles) fusion excitation functions [12].

process but also in one-neutron transfer or two-neutron transfer reactions followed by neutron evaporation. In [12, 13] we have subtracted the contribution due to the transfer by replacing the measured value for  ${}^{65}\text{Zn}$  with the one calculated using the statistical model. After this correction, the fusion excitation functions for  ${}^{6,4}\text{H} + {}^{64}\text{Zn}$ , shown in fig. 2, are rather similar within the errors and within the measured energy range. It seems that at this energies the presence of the halo structure does not imply particular effects on the fusion mechanism. We cannot say anything about the possible effects that the  ${}^6\text{He}$  valence neutrons could generate at energies below the Coulomb barrier, since the  ${}^4\text{He}$  data in [12, 13] do not cover the lower part of the energy range investigated for the  ${}^6\text{He} + {}^{64}\text{Zn}$  system.

### 3. – New ${}^4\text{He} + {}^{64}\text{Zn}$ experiment

**3.1. Activation technique.** – To investigate the role of the halo structure at energies lower than the Coulomb barrier we measured additional points in the fusion excitation function of  ${}^4\text{He} + {}^{64}\text{Zn}$  to cover the same energy range of the  ${}^6\text{He}$  data previously measured in [12, 13] and shown in fig. 2. This new experiment was performed at the Tandem accelerator of the Ruder Boskovic Institute in Zagreb with an average  ${}^4\text{He}$  beam current of about  $10^{11}$  pps. The reaction was measured at  $E_{\text{lab}} = 8.1, 9.2$  and  $10.1$  MeV. As in our previous experiments [12, 13] the fusion excitation function was measured using the off-line activation technique. In this experiment, for each beam energy it was irradiated one  ${}^{64}\text{Zn}$  target ( $540 \mu\text{g}/\text{cm}^2$ ) followed by a Nb catcher ( $1000 \mu\text{g}/\text{cm}^2$ ). We note that, as in the present experiment, where a fusion reaction is induced by a low-energy light projectile onto a medium-mass target, a large fraction of the produced evaporation residues does not have enough kinetic energy to exit the target and their direct detection is not possible. However, by choosing a suitable target, as in the present case, it is possible to obtain radioactive ER unstable against EC decay. We “detect” the ER by looking at the atomic X-rays emitted in their decay. The small fraction of residues emerging from the target is stopped in the  ${}^{93}\text{Nb}$  catcher placed behind the target. At the end of the irradiation time the activated target and catcher are placed close to a Si(Li) detector to measure the activity. The targets irradiated at the Zagreb Tandem were measured at the Laboratori Nazionali del Sud in Catania for about twenty days. One of the advantages of

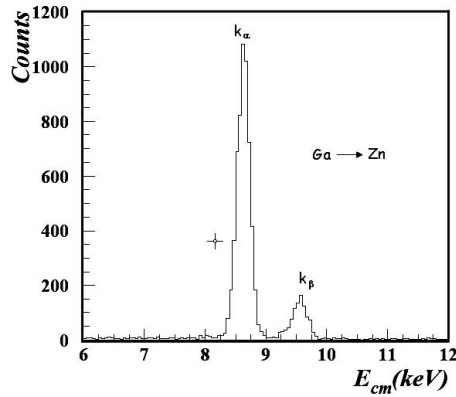


Fig. 3. – Typical X-ray spectrum measured off line for the reaction  ${}^4\text{He} + {}^{64}\text{Zn}$ . It is possible to distinguish two peaks which correspond to the  $K_\alpha$  and  $K_\beta$  X-ray emission of Zn.

this technique is the 100% intrinsic detection efficiency of the Si(Li) detector in the X-ray energy region of interest (7–11 KeV). Moreover, the atomic X-ray in this energy region can be detected with extremely low background. We note that X-rays due to the decay of heavy residues produced in the reaction of  ${}^4\text{He}$  with the Nb catcher contribute to an energy region of the X-ray spectrum different than the one of our interest and therefore do not represent a problem.

**3.2. Experimental results.** – In fig. 3 a typical X-ray off-line spectrum for the reaction  ${}^4\text{He} + {}^{64}\text{Zn}$  is shown. It corresponds to the target activated at the highest energy,  $E_{\text{lab}} = 10.1$  MeV. From the X-ray energy it is possible to identify the  $K_\alpha$  and  $K_\beta$  contribution due to the decay of the Ga into Zn. As one can see, the background level is very small when compared to the signal.

Characteristic X-ray energies only identify different elements but not different isotopes. However it is possible to discriminate isotopes by following the X-ray activity of the element as a function of time. In fig. 4, the activity curve for the Ga peak is shown.

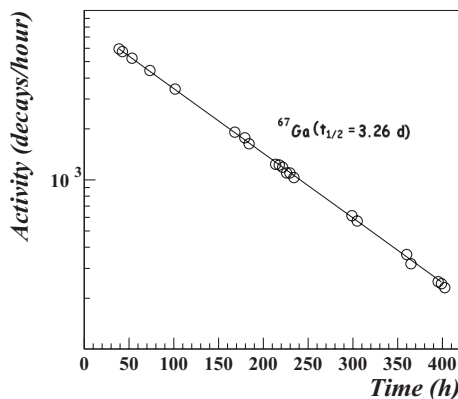


Fig. 4. – Activity curve for the  ${}^{67}\text{Ga}$  isotope extracted in the activation run.

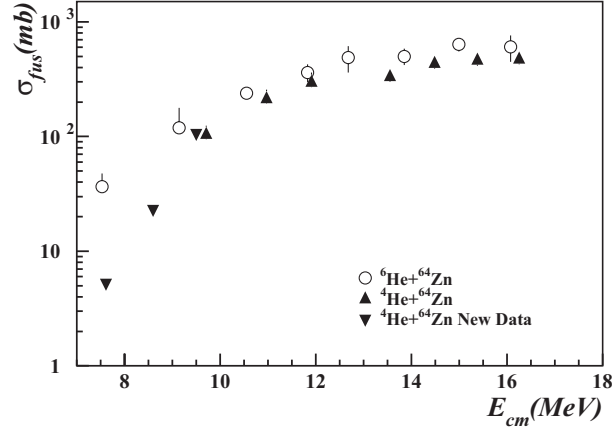


Fig. 5. –  ${}^6\text{He} + {}^{64}\text{Zn}$  (circles) and  ${}^4\text{He} + {}^{64}\text{Zn}$  (triangles) fusion excitation functions. Inverted triangles represent the present  ${}^4\text{He}$  data.

As one can see from the slope of the activity curve, only the contribution of the  ${}^{67}\text{Ga}$  isotope, having a half-life of 3.26 days, is present.

This is in agreement with the predictions of statistical-model calculations. In fact the only evaporation residues produced in the  ${}^4\text{He} + {}^{64}\text{Zn}$  fusion reaction at these energies are predicted to be  ${}^{67}\text{Ge}$  and  ${}^{67}\text{Ga}$ . The first one is a short-lived nucleus ( $t_{1/2} = 18$  minutes) and it decays by EC 100% into  ${}^{67}\text{Ga}$ . For this reason, after few hours, all produced  ${}^{67}\text{Ge}$  is transformed into  ${}^{67}\text{Ga}$ , therefore, we observe only this contribution.

For the above reason, the total fusion cross-section corresponds to the one measured for the longer-lived  ${}^{67}\text{Ga}$  ( $T_{1/2} = 3.26$  d) whose production cross-section can be extracted by using the following formula:

$$(1) \quad \sigma = \frac{A_{0exp}}{N_i N_t \lambda_0 K_\alpha \varepsilon_T},$$

where  $A_{0exp}$  is the experimentally measured activity at the end of the irradiation as obtained from the fit of the activity curve (fig. 4). This term is then corrected for the known  $K_\alpha$  fluorescence probability and for the detector efficiency ( $\varepsilon_T$ );  $\lambda_0$  is the decay constant;  $N_t$  is the number of target atoms per  $\text{cm}^2$  and  $N_i$  is the integrated beam current (*i.e.* the number of incident particles during irradiation). In fig. 5 the excitation functions for the present  ${}^4\text{He} + {}^{64}\text{Zn}$  data and for the previous data of  ${}^{4,6}\text{He} + {}^{64}\text{Zn}$  [12, 13] are shown. The consistency of the present  ${}^4\text{He}$  data with the ones of [12, 13] is confirmed by the good agreement of the two points at around 9.5 MeV.

As one can see, an enhancement of the fusion excitation function at energies below the Coulomb barrier in the case of  ${}^6\text{He}$  with respect the  ${}^4\text{He}$  one is observed. The enhancement effect for  ${}^6\text{He}$ -induced fusion shown in fig. 5, includes both the effect due to the larger  ${}^6\text{He}$  radius and the possible effects due to the coupling to other channels including break-up. However, from this comparison, it is not possible to know if the role of one of the two effects is more important than the other.

#### 4. – Conclusions

In the present paper, our previous comparison of fusion excitation functions for the systems  ${}^6,{}^4\text{He} + {}^{64}\text{Zn}$  around the Coulomb barrier [12, 13] has been extended to lower energies by measuring a new set of  ${}^4\text{He} + {}^{64}\text{Zn}$  fusion cross-sections. The results show an enhancement of the  ${}^6\text{He}$ -induced fusion cross-sections with respect to the one induced by  ${}^4\text{He}$  on the same target in the energy region around and below the barrier.

From the experimental data published so far, apparently contradictory conclusions on the presence of enhancement/suppression effects on fusion excitation functions around the barrier in collisions induced by halo nuclei have been reached by different authors. One has to notice, however, two important points: most of existing data do not really explore the region below the barrier with reasonable errors; different authors reached their conclusions by performing a different kind of analysis and this may affect the final result as discussed in [7]. Therefore, for a better understanding of the discussed topic new experimental data in the low energy region are surely needed as well as coherent analysis procedures of existing experimental data.

#### REFERENCES

- [1] CANTO L. F. *et al.*, *Phys. Rep.*, **424** (2006) 1.
- [2] HAGINO K. *et al.*, *Phys. Rev. C*, **61** (2002) 037602.
- [3] DIAZ-TORRES A. and THOMPSON J. J., *Phys. Rev. C*, **65** (2002) 024606.
- [4] ITO M. *et al.*, *Phys. Lett. B*, **37** (2006) 53.
- [5] KOLATA J. J. *et al.*, *Phys. Rev. Lett.*, **81** (1998) 4580.
- [6] DE YOUNG P. A. *et al.*, *Phys. Rev. C*, **58** (1998) 3442.
- [7] CANTO L. F. *et al.*, *Nucl. Phys. A*, **821** (2009) 51.
- [8] RAABE R. *et al.*, *Nature*, **431** (2004) 823.
- [9] PENIONZHKEVICH YU. E. *et al.*, *Eur. Phys. J. A*, **31** (2007) 185.
- [10] LEMASSON A. *et al.*, *Phys. Rev. Lett.*, **103** (2009) 232701.
- [11] SIGNORINI C. *et al.*, *Nucl. Phys. A*, **735** (2004) 329.
- [12] DI PIETRO A. *et al.*, *Phys. Rev. C*, **69** (2004) 044613.
- [13] DI PIETRO A. *et al.*, *Eur. Phys. J. ST*, **150** (2007) 15.